ELSEVIER

Journal of Nuclear Materials 307–311 (2002) 439–443

journal of nuclear materials

www.elsevier.com/locate/jnucmat

Post-irradiation annealing of neutron irradiated CuCrZr

D.J. Edwards [a,*], B.N. Singh [b], Q. Xu [c], P. Toft [b]

[a] Pacific Northwest National Laboratory, Department of Structural Materials Development, MSIN P8-15, Richland, WA, 99352, USA

[b] Risø National Laboratory, Department of Materials Research, DK-4000 Roskilde, Denmark

[c] Research Reactor Institute, Kyoto University, Osaka 590-0494, Japan

Abstract

The effect of post-irradiation annealing at 300 °C for 50 h on the microstructure and mechanical properties of CuCrZr irradiated to 0.2 and 0.3 dpa at 100 °C has been evaluated. The post-irradiation annealing removes the yield point phenomenon, lowers the strength and improves the ductility and work hardening of the material. It does not, however, completely remove the effects of irradiation as the annealed material is still considerably stronger and less ductile than the unirradiated CuCrZr alloy. The removal of the yield point phenomenon is attributed to a decrease in raft formation and dislocation decoration, weakening the dislocation pinning and allowing more homogeneous generation of dislocations within the material. The segregation of solute additions, impurities and transmutation elements as well as precipitation at dislocation segments and loops needs to be further investigated to fully understand the mechanical properties.

1. Introduction

Low temperature radiation hardening in metals and alloys is an important phenomenon that has been studied for over 40 years (e.g. see [1–3]). When metals and alloys are irradiated at temperatures below the recovery stage V, substantial increases in strength and drastic loss of ductility and work hardening ability occur at relatively low neutron doses, a matter of serious concern in fusion reactor applications. A recent review by Singh et al. [4] reveals that radiation hardening in metals and alloys is due to the evolution of the fine-scale defect microstructure, which ultimately leads to fundamental changes in the manner in which the material deforms.

For fusion applications, copper and copper-based alloys have been evaluated for use as heat sink materials in the plasma facing components such as the first wall and divertor. Recent irradiation experiments have shown that pure copper and copper-based alloys exhibit substantial radiation hardening and loss of ductility, the degree of which depends on their composition, initial processing and the irradiation temperature and dose [5–7]. In the case of pure copper and precipitation-strengthened CuCrZr, the radiation hardening can be very severe at irradiation temperatures below ≈200 °C. Radiation hardening and the detrimental loss of ductility cannot be easily prevented without changing the nature of the metal or alloy itself through additional alloying or processing. However, one possible solution arises from the bakeout thermal treatments that have been contemplated in order to improve the vacuum of the plasma chamber. One proposed bakeout treatment is 300 °C for 50 h, a temperature which is high enough to possibly allow recovery of the irradiation-induced defect microstructure in pure copper and its alloys. Singh et al. [7] explored this possibility by irradiating pure copper at 100 °C and then annealing at 300 °C for 50 h. Their results demonstrated that post-irradiation (PI) annealing at 300 °C for 50 h was only partially successful in restoring the properties of irradiated OFHC copper to its unirradiated state.

* Corresponding author.
E-mail address: dan.edwards@pnl.gov (D.J. Edwards).

0022-3115/02/$ - see front matter
PII: S0022-3115(02)01037-1

In this paper we will present tensile data and microstructural data from a companion experiment illustrating the behavior of a precipitation-hardened CuCrZr alloy in both the as-irradiated and post-irradiation annealed conditions. The effect of annealing on the microstructure and mechanical properties will be compared to the results reported earlier on the unirradiated and the as-irradiated samples [5,6].

2. Materials and experimental procedure

Tensile specimens of CuCrZr (Cu-0.8% Cr, 0.07% Zr, 0.01% Si) were irradiated at 100 °C in the DR-3 reactor at Risø National Laboratory to displacement levels of 0.2 and 0.3 dpa (NRT). Prior to irradiation, the specimens were divided into two sets, one set being given a prime ageing treatment (heat treatment E) and the other a simulated bonding thermal cycle treatment (heat treatment B) [5,6]. The prime ageing consisted of solution annealing at 950 °C for 1 h, water quenching, then ageing at 475 °C for 30 min and water quenching. The simulated bonding cycle consisted of heat treatment E followed by a solution annealing treatment of 950 °C for 30 min, furnace cooled, then re-aged at 475 °C for 30 min followed by furnace cooling.

Tensile specimens were irradiated with a neutron flux of 2.5×10^{17} n/m^2 ($E > 1$ MeV) corresponding to a displacement rate of $\sim 5 \times 10^{-8}$ dpa/s. A subset of the irradiated specimens was given a post-irradiation annealing treatment at 300 °C for 50 h in vacuum ($<10^{-8}$ bar). Tensile specimens were available for both the as-irradiated and post-irradiation annealed conditions at 0.2 and 0.3 dpa, but for the corresponding microstructural characterization, no specimens were available for the as-irradiated 0.2 dpa condition. Specimens of the unirradiated, as-irradiated and post-irradiation annealed specimens were tensile tested at 100 °C in vacuum ($<10^{-7}$ bar) at a strain rate of 1.2×10^{-3} s^{-1}. The test temperature was reached within 30 min.

The microstructure of various samples in the as-irradiated, irradiated and annealed conditions and after deformation was investigated. For the post-deformation microstructural characterization, 2-mm wide strips were cut from the gauge length of the tensile specimens after they fractured during testing. The 2-mm wide strips included the fracture surface to ensure that the deformed microstructure was examined. Specimens were prepared by electropolishing the specimens using a 25% perchloric, 25% ethanol and 50% water electrolyte. Microstructural characterization of the different specimen conditions was conducted by transmission electron microscopy in a JEOL 2000FX microscope. The details of the techniques used to characterize the microstructure have been provided in detail in earlier reports [5,6].

3. Results

3.1. Microstructural analysis

The unirradiated microstructure consists of a high density of small spherical precipitates ranging from 0.36 to 0.59×10^{23} m^{-3} in density with an average size of 2.3–2.9 nm [5,6]. The dislocation density is relatively low ($<10^{12}$ m^{-2}) and the grain size is approximately 30 μm due to the initial solution annealing treatment. A very low density of large Cr-rich particles are present in the grain interiors and at grain boundaries. The nature of the dispersion of small precipitates remains unclear, but are thought to be primarily small Cr-rich precipitates with some Cu–Zr precipitates present [5,6].

Irradiation at 100 °C coarsens the precipitate microstructure, lowering the density slightly (to $\simeq 0.26 \times 10^{23}$ m^{-3}) and increasing the average size of the precipitates in both heat treatments (HT B: 4.5 nm, HT E: 5.6 nm). The microstructure contains a high density of SFTs typical of irradiated microstructures in copper and some of its alloys (see Table 1). From the size and density, the number of vacancies contained in the SFTs has been calculated and is given in Table 1 (for details see [7]). Agglomerations of small clusters appear to have formed a raft-like structure of loops and some dislocation segments at 0.3 dpa, similar to that observed in OFHC copper [7].

Post-irradiation annealing produces a noticeable shift to a larger average SFT size and lower density when compared to the as-irradiated condition. Size distributions showing a comparison between the SFT in the as-irradiated and the post-irradiation annealed case are provided in Fig. 1. Note that there is only a little or no difference in the SFT size between the 0.2 and 0.3 dpa specimens in the post-irradiation annealed condition. The precipitate microstructure after annealing exhibits substantial changes compared to the as-irradiated case. Preliminary results suggest that the precipitates are not present in as high a density after annealing, but further work is needed to understand the details of the changes

Table 1
SFT characteristics and the number of vacancies contained in the SFTs, N_V, in the CuCrZr alloy

Heat treatment	SFT density ($\times 10^{23}$ m^{-3})	SFT size (nm)	N_V (10^{25} m^{-3})
As-irradiated			
(HT B)	5.5	2.2	3.5
(HT E)	5.7	2.1	3.3
Post-irradiation annealed (300 °C for 50 h)			
(HT B) 0.3 dpa	2.0	3.4	3.0
(HT E) 0.2 dpa	2.3	3.4	3.5
(HT E) 0.3 dpa	2.1	3.5	3.4

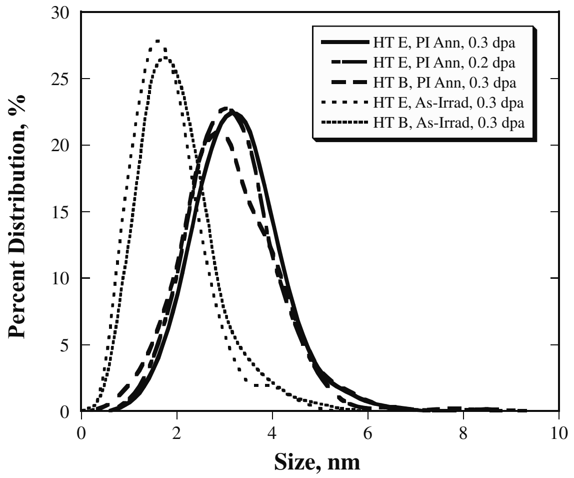

Fig. 1. Size distributions of the SFT for both heat treated conditions are shown illustrating the effect of post-irradiation annealing at 300 °C for 50 h. PI annealing shifted the size distributions to a larger average size.

after annealing. After post-irradiation annealing, the agglomeration of loops present in the as-irradiated samples have coalesced to yield a network of dislocation loops and line segments, with a total line density of $\simeq 10^{14}$ m^{-2}. A comparison of the loop microstructure in the as-irradiated and post-irradiation annealed heat treatment E sample at 0.3 dpa is provided in Fig. 2.

It is interesting to note that the number of vacancies (N_V) contained in the SFTs does not change due to post-irradiation annealing (see Table 1). Furthermore, the values of N_V in the as-irradiated CuCrZr alloy are very similar to that in the as-irradiated OFHC copper (at 100 °C to 0.3 dpa). However, the post-irradiation annealing at 300 °C for 50 h yields a somewhat higher value of N_V in the OFHC copper than that in the CuCrZr alloy [7].

3.2. Tensile results

A comparison of the tensile behavior of the as-irradiated and the post-irradiation annealed conditions for the HT E specimens is shown in Fig. 3. Irradiation to 0.2 or 0.3 dpa causes a significant increase in the yield

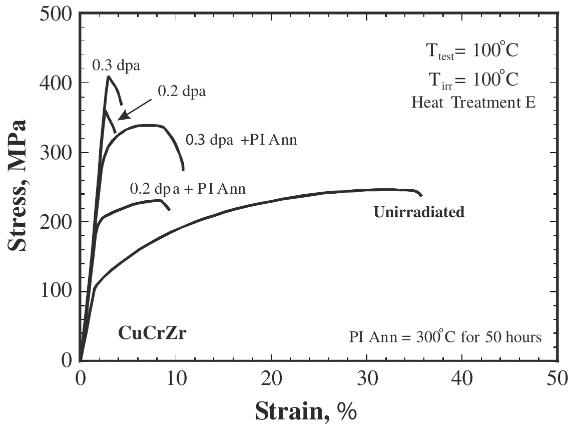

Fig. 3. Tensile curves are shown illustrating the effect of post-irradiation annealing on the deformation behavior of irradiated CuCrZr in the HT E condition. PI annealing lowers the strength, removes the yield drop and restores a fraction of the ductility and work hardening.

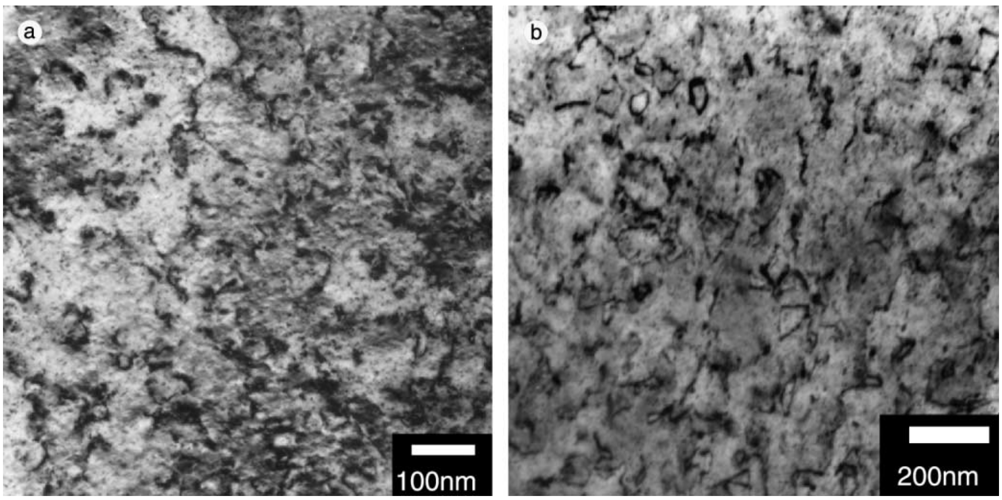

Fig. 2. Microstructure of CuCrZr (HT E) neutron irradiated at 100 °C to 0.3 dpa in the (a) as-irradiated condition and (b) irradiated and annealed (at 300 °C for 50 h) conditions, showing the presence of small loops and raft-like structures of SIA loops in (a) and dislocation segments and larger loops in (b).

strength of the CuCrZr, but reduces the uniform elongation and work hardening ability of the material to zero. There are no distinct yield and ultimate stress, rather only a maximum stress beyond which the material becomes unstable in tension and begins necking. In other words, after reaching the upper yield point, the material suffers from a drastic yield drop and plastic instability that rapidly leads to necking and failure. The post-irradiation annealing removes the yield point behavior and restores some uniform elongation and work hardening ability to the irradiated alloy at both doses. However, the post-irradiation annealed specimens are still considerably stronger and less ductile than the unirradiated specimens. The tensile behavior for the 0.2 and 0.3 dpa condition both before and after annealing are distinctly different, indicating that there is some feature in the microstructure that influences the tensile properties in a dose dependent manner. The HT B condition exhibits a similar behavior as that observed for the HT E condition.

3.3. Post-deformation microstructure

Various features of the post-deformation microstructure of the as-irradiated and post-irradiation annealed CuCrZr alloy have been examined using TEM. Because of the space limitation, only the salient features are described below, a detailed description will be given in a later publication.

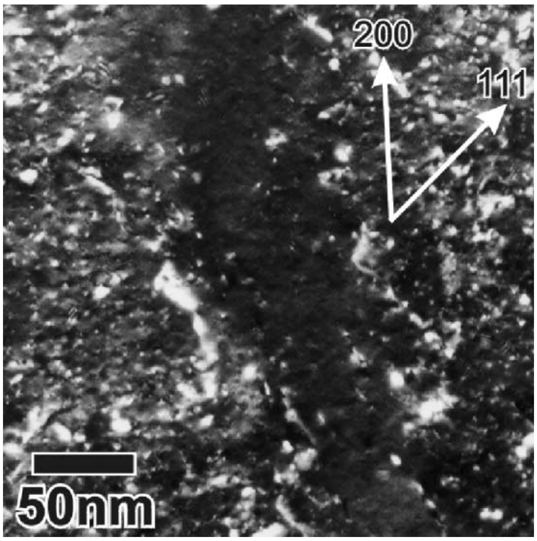

Fig. 4. An example of a channel shown in the as-irradiated condition shows that deformation occurs in an inhomogeneous fashion. The channels contain only a small fraction of the defect clusters and precipitates present in the material surrounding the channels. Note that there is no evidence of dislocation generation and homogeneous deformation.

The dominating feature of the deformed microstructure in the case of the as-irradiated condition is the presence of cleared channels. The observations show that the deformation occurs in a localized fashion such that dislocation generation and motion are restricted to the cleared channels only. An example of such a cleared channel is shown in Fig. 4. This behavior is fully consistent with the tensile behavior shown in Fig. 3. As can be seen in Fig. 4, most of the defect clusters and a substantial fraction of the precipitates have been destroyed by the successive passage of dislocations in the channels. The cleared channels are commonly initiated at points of singularities such as inclusions, twin and grain boundaries. In the PI annealed case, deformation occurs in a much more homogeneous manner with very few ill-defined channels.

4. Discussion

The results presented here demonstrate that the post-irradiation annealing at 300 °C for 50 h is only partially successful in removing the effects of radiation hardening. The microstructure characterization reveals a number of issues that affect the annealing response of the material. First, the size distributions of the SFT in the as-irradiated conditions appear to be insensitive to the starting condition of the alloy (HT E versus HT B) as shown in Fig. 1. This does not change after annealing since the size distributions remain essentially identical for the two conditions. Secondly, the total number of vacancies does not change appreciably after annealing, indicating that annealing does not lead to the annihilation of vacancies, instead, the SFTs have coarsened somewhat under these annealing conditions. Furthermore, the SFT in the CuCrZr alloy behave in a similar manner to those observed in the post-irradiation annealing experiment on OFHC Cu reported previously by Singh et al. [7]. In both materials the SFT density decreases during annealing and the average size increases, however, these changes are not quite as large in the CuCrZr as they are in the OFHC copper. In general the presence of the precipitates and alloying additions do not appear to have a drastic effect on the SFT microstructure when compared to the case of the OFHC copper.

PI annealing (300 °C for 50 h) removes the yield drop and improves the ductility and work hardening in both CuCrZr and OFHC copper, but not to the same degree. The density and average size of SFT reported for the PI annealed OFHC copper at 0.2 and 0.3 dpa are again similar to that reported in this study for the PI annealed CuCrZr, so the higher strength of the CuCrZr cannot be directly related to just the SFT microstructure. The measured dislocation densities in the annealed CuCrZr and OFHC copper are also similar for both materials. In addition, post-irradiation annealing produces a considerable disparity in the yield strength of the CuCrZr irradiated to 0.2 and 0.3 dpa, yet there is no discernible difference in visible defect microstructures for the two conditions that explains the different levels of strength after annealing. These facts indicate that not all of the features of the microstructure that contribute to strengthening have been completely accounted for in our investigation, as will be discussed below.

Radiation-induced segregation of the Cr, Zr and other impurities (plus any transmutation elements such as Ni and Zn produced during irradiation) to defect clusters and dislocations may be responsible in part for the higher level of strength in the CuCrZr alloy. Whether this changes the effective 'strength' of the individual obstacles, produces a Cottrell atmosphere or leads to precipitation on the defect clusters and dislocations, or is a combination of both is not yet clear. Singh et al. [7] concluded that in the case of irradiated OFHC copper, the pre-existing dislocations were pinned by small loops produced during irradiation, and that the yield drop was the result of dislocations generated from local singularities at internal boundaries and inclusions in lieu of the normal dislocation generation mechanisms (Frank–Read sources). The disappearance of the yield drop after annealing was therefore interpreted to be a consequence of the removal of the atmospheres of loops, allowing the other, more widely spaced features in the microstructure (SFTs, loops, and dislocations) to control the initiation of plastic flow and subsequent work hardening behavior. The same argument can be used here for the CuCrZr since the changes in strength do not appear to completely follow the observed microstructure. However, compared to the OFHC copper, the added complication exists that the presence of alloying additions will alter how the dislocations interact with the microstructure. Further, the microstructural characterization does not show precisely how the alloying additions affect the evolution of the post-irradiation annealed microstructure.

5. Conclusions

The present results and their discussion lead to the following conclusions:

(a) the increase in the yield strength and the appearance of the yield drop followed by the plastic instability in the as-irradiated CuCrZr alloy seems to be related to the formation of the raft-like microstructure and the decoration of the grown-in dislocations by small SIA loops and probably the segregation of impurity atoms which may lead to precipitation on the dislocations,

(b) immediately beyond the upper yield stress, the material seems to deform almost entirely in a localized fashion in the form of cleared channels,

(c) post-irradiation annealing at 300 °C for 50 h eliminates the occurrence of the yield drop and plastic instability and enables the material to work harden. This indicates that the raft formation and dislocation decoration have been weakened due to annealing and are no longer controlling the deformation behavior,

(d) it is somewhat surprising that annealing at 300 °C for 50 h does not seem to cause any reduction in the total number of vacancies contained in the stacking fault tetrahedra,

(e) effects of impurity segregation at dislocation segments and loops on mechanical properties need to be investigated further.

Acknowledgements

The present work was partly funded by the European Fusion Technology Programme. The authors wish to thank B.F. Olsen, N.J. Pederson and J.L. Lindbo. D.J. Edwards would like to thank Risø National Laboratory for the support and assistance during his visit. His work was also partly supported by the US Department of Energy under contract DE-AC06-76RLO 1830 with the Battelle Memorial Institute at the Pacific Northwest National Laboratory.

References

[1] A. Seeger, in: Proceedings of the 2nd UN International Conference on Peaceful Uses of Atomic Energy, Geneva, vol. 6, 1958, p. 250.
[2] T.H. Blewitt, R.R. Coltman, R.E. Jamison, J.K. Redman, J. Nucl. Mater. 2 (4) (1960) 277.
[3] M.J. Makin, Rad. Eff. 37 (1965) 627.
[4] B.N. Singh, A.J.E. Foreman, H. Trinkaus, J. Nucl. Mater. 249 (1997) 103.
[5] B.N. Singh, D.J. Edwards, M. Eldrup, P. Toft, J. Nucl. Mater. 249 (1997) 1.
[6] D.J. Edwards, B.N. Singh, P. Toft, M. Eldrup, J. Nucl. Mater. 258–263 (1998) 978.
[7] B.N. Singh, D.J. Edwards, P. Toft, J. Nucl. Mater. 299 (2001) 205.